SCHEUERMANN'S DISEASE AS A MODEL DISPLAYING THE MECHANISM OF VENOUS OBSTRUCTION IN THORACIC OUTLET SYNDROME AND MIGRAINE PATIENTS: MRI AND MRA

James D. Collins, Ernestina H. Saxton, Theodore Q. Miller, Samuel S. Ahn, Hugh Gelabert, and Alfred Carnes

Scheuermann's Disease: An MRI MRA Model Displaying the Mechanism of Venous Obstruction in Thoracic Outlet Syndrome (TOS) and Migraine Patients. Collins JD, Saxton EH, Miller TQ, Ahn SS, Galebert H, Carnes AE Departments of Radiological Sciences Neurology and Vascular Surgery, UCLA

Kyphosis of the thoracic spine rotates the scapulae anterior laterally, clavicles and subclavius muscles anteriorly, displaces the manubrium posteriorly, which increases the slope of the first ribs. This increases tension on the anterior scalene muscles and the neurovascular bundles which causes brachial plexopathy (TOS). Scheuermann's disease (spinal osteochondrosis; juvenile kyphoscoliosis) is a disorder which consists of vertebral wedging, endplate irregularity and narrowing of the intervertebral disk space causing kyphosis of the thoracic spine and may also involve the lumbar space. It occurs at puberty and involves both male and females. Abduction external rotation of the upper extremities (arms overhead) posterior inferiorly rotate the clavicles and the subclavius muscles which enhances tension on the venous drainage and neurovascular supply that diminishes venous return. This triggers complaints of thoracic outlet syndrome (TOS) and migraine headache. Bilateral magnetic resonance imaging (MRI) demonstrates compressing abnormalities of the brachial plexus. Five patients with Scheuermann's disease were imaged with the 1.5 Tesla magnet (Signa; General Electric Medical Systems, Milwaukee, WI) 3-D reconstruction MRI. T1W and T2W pulse sequences were performed in the coronal, transverse, transverse oblique, sagittal, and coronal abduction external rotation planes using 4 mm slice thickness and 512 × 256 matrix size. Water bags were used to enhance the signal to noise ratio. Magnetic resonance angiography (MRA) 2-D Time Of Flight (TOF) was obtained to evaluate perfusion of the brachial plexus. MRI and MRA captured sites of brachial plexus compression for anatomic display. One patient was selected for this presentation, which demonstrates the compression of the brachial plexus and venous obstruction which triggered complaints of thoracic outlet syndrome. (*J Natl Med Assoc.* 2003;95:298–306.)

Key words: MRI ◆ MRA ◆ migraine, nerves imaging ◆ neuropathy ◆ brachial plexus ◆ Scheuermann's disease ◆ thoracic outlet syndrome

INTRODUCTION

Magnetic resonance multi-plane imaging allows bilateral display of the thorax and brachial plexus in the supine position. This feature gave us an opportunity to image and study the brachial plexus[1].

The brachial plexus lies within the fascial planes of the neck and axilla, which is routinely displayed on MRI of the thorax and shoulder girdle[2]. Abnormalities of the brachial plexus result from problems with the cervico-thoracic

© 2003. Departments of Radiology (J.D.C., T.Q.M., A.C.), Neurology (E.H.S), and Vascular Surgery (H.G., S.S.A), University of California at Los Angeles, USA. Presented at the National Medical Association 104th Annual Scientific Program, Convention and Scientific Assembly, Convention center, Las Vegas, Nevada, August 11, 1999 and at the Federation of American Societies for Experimental Biology , San Diego, California, April 15–18, 2000. Correspondence should be directed to James D. Collins Department of Radiological Sciences, University of California, Los Angeles, 1083 Le Conte Ave. Los Angeles, CA 90095–0001.

segments of the vertebral column, the first rib, clavicle, vascular supply, Manubrium sterni and soft tissues[3]. In most individuals, the fascial plane spacing between soft tissues and osseous structures is adequate to perform routine functions without compromising their neurovascular bundles. Studies by Sunderland in 1945 and Dyke et al in 1984 suggest that pathology involving peripheral nerves alters fascial planes[4,5]. Acute or chronic changes alter adjacent tissues, thereby compromising the vascular supply of the peripheral nerves[6]. This results in patients presenting with clinical symptoms of thoracic outlet syndrome (TOS): tingling, numbness, pain (face, shoulder, upper and lower extremities, back, and abdomen); visual and auditory changes; syncope and headache (6 FASEB 2002).

Knowledge of normal surface and landmark anatomy is important for interpretation of MRI and MRA studies in patients with brachial plexus injury[7]. The brachial plexus nerve roots pass with the subclavian artery to form a neurovascular bundle between the anterior and middle scalene muscles on the first ribs (scalene triangles). The scalene muscles arise from the cervical segments of the vertebral column, insert and, in part, support the curved, flat first ribs. The first ribs slope obliquely attaching to the manubrium to form most of the thoracic inlet. The slope of the first ribs changes with respiration, scoliosis, and kyphosis of the thoracic spine and affects those structures crossing the first rib, particularly the subclavian veins[7].

Kyphosis of the thoracic spine occurs in Scheuremann's disease (spinal osteochondrosis; adolescent kyphoscoliosis), which is an abnormality in the shape and size of the vertebral bodies of the thoracic and lumbar spine[8]. Vertebral bodies assume wedge shape deformities and disk spaces narrowing which contribute to kyphosis of the thoracic spine and abnormal alignment of the shoulder girdle, which alter fascial planes (Figs 1,2).

Thoracic outlet syndrome (brachial plexopathy) occurs in patients with Scheuremann's disease and other disorders of the cervicothoracic spine[9,10]. The authors have chosen Scheuermann's disease as a classic presentation in a young patient of brachial plexopathy secondary to kyphosis of the thoracic spine and rounding of the shoulders. Bilateral magnetic resonance imaging (MRI) and angiography (MRA) of the brachial plexus and peripheral nerve make it possible to demonstrate the relationship of nerves to their surrounding landmark anatomy in Scheuremann's disease patients with TOS.

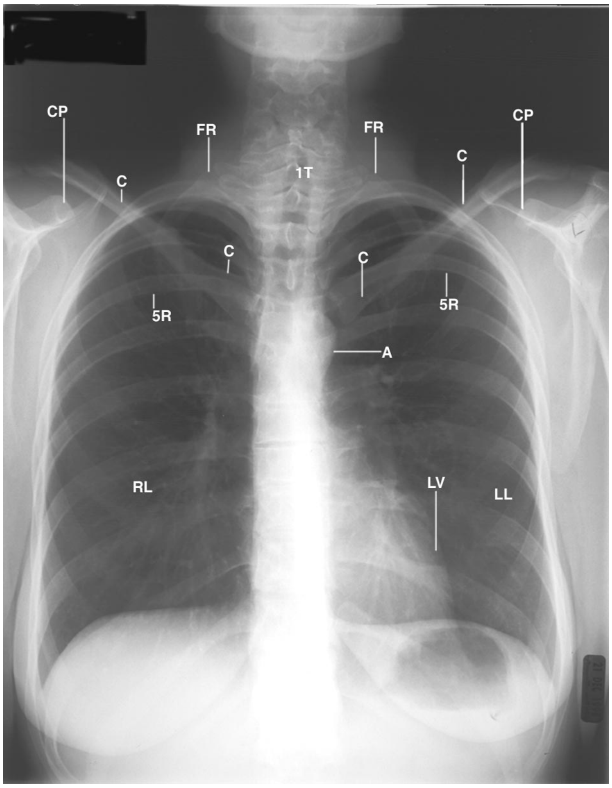

Figure 1. PA upright chest radiograph displays the forward shift of the shoulders with anterior rotated clavicles (C) low over acute sloping first ribs (FR), and the anterior lateral rotated coracoid processes (CP), reflecting bilateral round shoulders. The heads of the clavicles (C) are below the fifth posterior ribs (5R). Right and left lung (RL,LL), aorta (A), first thoracic vertebra (1T).

All MRI and MRA sequences were cross-referenced in order to arrive at an accurate diagnosis. It is not possible to present all of the acquired images; the images selected for this presentation were annotated and best display

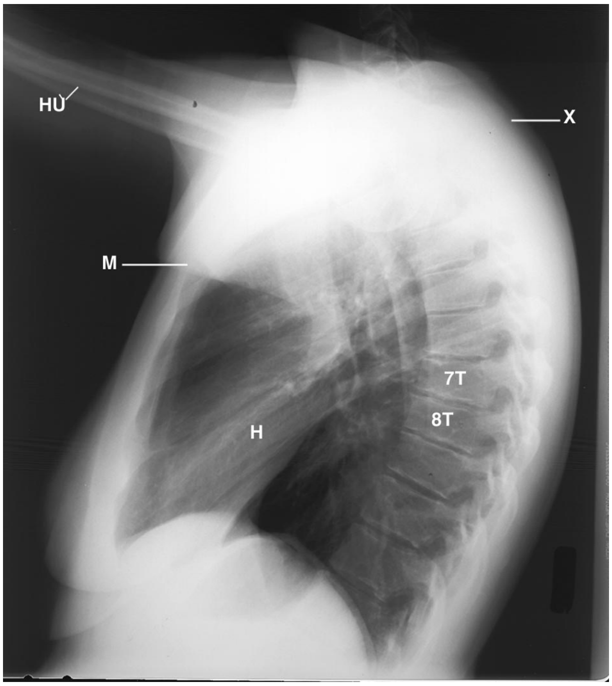

Figure 2. Lateral upright chest radiograph displays kyphosis of the thoracic spine and rounding of the shoulders (X) with anterior wedging of thoracic vertebrae (7T, 8T). "Pancake shaped" heart (H), humerus (Hu), Manubrium (M).

the pathologic changes that occur in costoclavicular compression of the brachial plexus.

METHODS AND MATERIALS

Plain chest radiographs (PA and lateral) are obtained and reviewed prior to the MRI. The procedure is discussed and the patient examined. Respiratory gating is applied throughout the procedure to minimize motion artifact. The patient is supine in the body coil, arms down to the side and imaging is monitored at the MRI station. Magnetic resonance images are obtained on the 1.5 Tesla GE Signa MR scanner (GE Medical Systems, Milwaukee, Wisconsin). A body coil is used and intravenous contrast agents are not administered. A water bag is placed on the right and the left side of the neck to increase signal to noise ratio for high resolution imaging. A full field of view (44 cm) of the neck and the thorax is used. to image both supraclavicular fossae. Contiguous (4 mm) coronal, transverse (axial), oblique transverse, sagittal, and abduction external rotation (of the upper extremities) T1-weighted images, and 2D Time Of Flight (TOF) MRA are obtained. If there is clinical evidence of scarring, tumor and/or lymphatic obstruction, Fast Spine Echo T2-weighted images are selectively obtained. The parameters for acquiring each sequence have been published[1,11,12]

CASE HISTORY

This was a 21-year-old right handed female with the diagnosis of Scheuermann's disease. She complained of headache with left upper extremity pain, tingling and numbness radiating into the left forearm, elbow and hand; mild tingling and numbness in the right hand; blurred vision and dots in the visual fields; neck pain radiating down into the coccyx, and ringing in ears. Elevating her left arm above shoulder height and combing her hair aggravated her symptoms. Symptoms began six months prior to evaluation by her referring neurologist, and were thought to be the result of prolonged typing.

Physical examination revealed the bent forward neck and the "hunched-up" rounding of her shoulders, left higher than right, and kyphosis of the thoracic spine. Swelling and tenderness were detected over the left supraclavicular fossa. Neurological examination revealed negative Spurling's maneuver; negative Lhermitte's sign and Tinel's sign over the median and ulnar nerves at the wrist and elbow. Radial pulses were present on abduction external rotation of the upper extremities. Roos' test was positive on the left and negative on the right. Tinel's sign in the supraclavicular fossa was negative.

The requesting neurologist suspected left thoracic outlet syndrome (TOS), with denervation of the left ulnar nerve by SSEP testing, not demonstrated on the right. Upper extremity electromyogram (EMG) and nerve conduction velocity study (NCV) indicated no evidence of left or right cervical or brachial plexopathy; no left or right carpal tunnel, Guyon's, and cubital tunnel syndromes, and no peripheral neuropathy. Because of suspected thoracic outlet syndrome, the neurologist requested bilateral MRI/MRA of the brachial plexus to determine the site(s) of brachial plexus compression.

The PA chest radiograph (Fig.1) displayed the "hunched up" round shoulders; heads of the anterior rotated clavicles over the posterior 5th intercostal spaces; right first rib higher than left; normal clear lungs, and small heart. The lateral chest radiograph (Fig. 2) displayed the thin narrow thorax; forward shift (kyphosis) of the thoracic spine; mild compression of thoracic vertebrae (7T,8T), and small heart (H) with round shoulders (X). The arms (HU) were near horizontal, because of expressed pain. It was concluded from the chest radiographs that she had bilateral round shoulders accentuated by kyphosis of the thoracic spine, and anterior wedging of the thoracic vertebrae.

The coronal MRI sequence of the brachial plexus displayed drooping of the small left shoulder and low left first rib as compared to the right (Figs 3A,B). The manubrium sloped left to the smaller hemithorax, tense flat subclavian arteries and binding nerve roots on the first ribs, left lower than right. The acute descent of the clavicles with subclavius muscles compressed (costoclavicular compression) the bicuspid valves[13] within the bulbous expanded subclavian veins and the right internal jugular vein, reflecting decrease venous return (Fig. 3B)[14], left greater than right. Residual Thymus gland was present within the thymic capsule.

The transverse MRI sequence cross referenced the coronal sequence to display the clavicles and subclavius muscles compressing the bicuspid valves within the subclavian veins against the anterior scalene muscles on the first ribs, left greater than right, and the narrow fascial planes of the supraclavicular fossa (Fig. 4). The manubrium sloped left to the smaller hemithorax. The head of the right clavicle compressed the right external jugular vein (not displayed) as it joined the compressed brachiocephalic vein (BRV). The dilated vertebral vein (VV) was compressed against the pleura. The right sternocleidomastoid muscle (STM) and

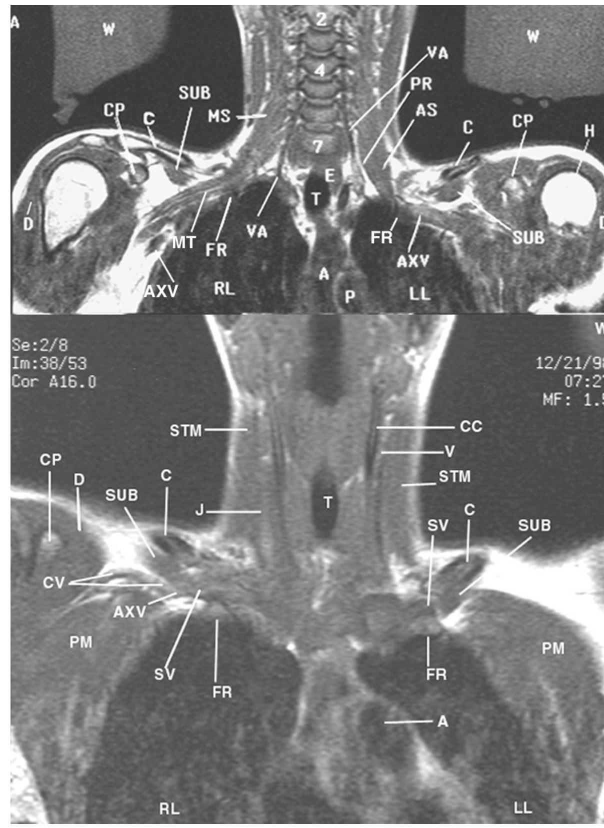

Figure 3(A,B). These coronal MRI images display the middle (Fig. 3A) and anterior (Fig. 3B) levels of the thorax. The left shoulder droops with the anterior rotated left clavicle (C) and subclavius (SUB) muscle closer to the lower first left rib (FR) as compared to the right (Figs A,B). Figure 3B displays the right clavicle and subclavius muscle compressing the subclavian vein (SV) as the cephalic vein (CV) joins the axillosubclavian vein (AXV). Aorta (A), common carotid and pulmonary arteries (CC,P), coracoid process (CP); anterior scalene, deltoid, pectoralis major, sternocleidomastoid muscles (AS,D,PM,STM); coracoid process (CP), esophagus (E), humerus (H), jugular vein (J), left and right lungs (LL,RL), middle trunk (MT), Trachea (T), Phrenic and vagus nerves) (PR). vertebral artery (VA), cervical vertebrae[2,4,7]

large anterior scalene muscle (AS) compressed the internal jugular vein (J).

The left and right transverse oblique sequences (not displayed) cross referenced and confirmed the coronal and transverse sequences above.

The left sagittal sequence cross referenced the above sequences to display the thin subcutaneous tissues, narrow thorax, and forward

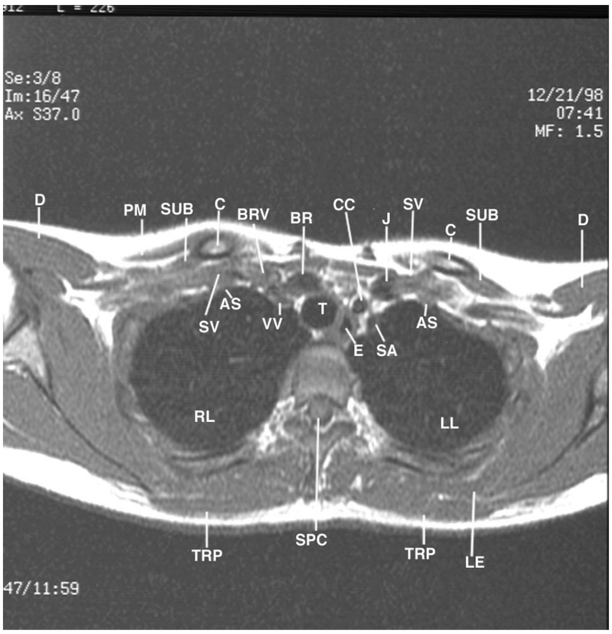

Figure 4. The transverse MRI cross references Figure 3 to display the dilated vertebral vein (VV) invaginating the pleura adjacent to the compressed brachiocephalic vein (BRV) and costoclavicular compression of the narrow fascial planes posterior to the clavicles. Gray signal intensity subclavian (SV), asymmetric clavicles (C) with subclavius muscles (SUB) left posterior to right, and the dilated right vertebral vein reflect decrease venous return. Brachiocephalic artery and common carotid arteries (BR,CC), esophagus (E), jugular vein (J), left and right lungs (LL,RL), spinal cord (SPC), trachea (T), vagus nerve (V); anterior scalene, deltoid, levator scapulae, pectoralis major, sternocleidomastoid, trapezius muscles (AS, D, LE, PM, STM, TRP).

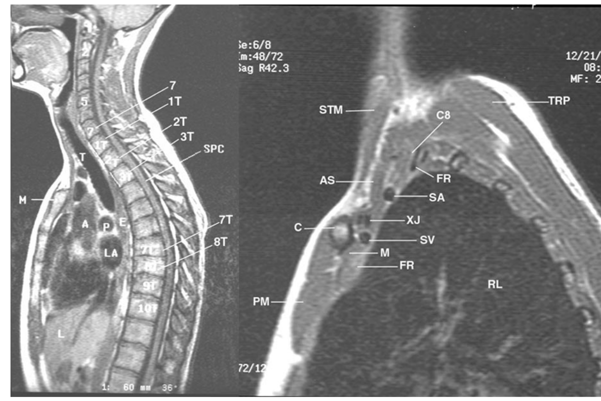

Figure 5(A,B). These images display the sagittal plane at the middle level of the cervicothoracic spine (Fig.5A) and to the right of midline within the right scalene triangle (Fig.5B). Figure 5A displays the forward shift of the cervicothoracic vertebrae, 7-T3, 36 degrees forward (left) off the zero degree vertical axis, and the anterior wedge shaped deformity of the thoracic vertebrae (7T,8T) reflecting rounding of the shoulders and kyphosis of the thoracic spine in the supine position. Figure 5B displays the anterior rotated clavicle in close proximity to the subclavian vein (SV). Backward manubrium (M) accentuates the narrow thorax. Aorta (A), esophagus (E), trachea (T), anterior scalene, sternocleidomastoid, pectoralis major, right lung (RL), trapezius muscles (AS,STM,PM,TRP), spinal cord (SPC), fifth and seventh cervical vertebrae[5,7]; thoracic vertebrae (1T-3T, 7T, 8T), eighth cervical nerve roots (C8).

shift of the cervicothoracic vertebrae (C7-T3) accentuating the round shoulders (Fig. 5A). The near vertical anterior scalene muscle with the anterior rotated clavicle and the subclavius muscle were in close proximity to the junction of the internal jugular and subclavian veins on the pleura secondary to the increased slope of the first rib. The subclavian artery and binding nerve roots were obscured by the gray signal intensity of the middle scalene muscle. The high signal intensity (white) cephalic vein, at the junction of the deltoid and pectoralis major muscle reflected decreased venous return.

The right sagittal sequence cross referenced the coronal and transverse sequences to confirm the anterior rotated clavicle (C) in close proximity to the larger right subclavian (SV) and external jugular veins (XJ); compression of the brachiocephalic vein at its junction with the vertebral vein (Fig.4); near vertical anterior scalene muscle (AS) between the subclavian vein (SV) and artery (SA), on the pleura with the binding nerve roots (Fig. 5B); compression of the right internal jugular vein, and mild costoclavicular compression of the right axillo-subclavian vein and artery (not displayed).

The 2D TOF MRA (stacked image, Fig. 6A) displayed the anterior bowed right and left neurovascular supply (right anterior to the smaller left) reflecting round shoulders; tense compression of the second division of the subclavian arteries (SA), left greater than right, and the asymmetric compressed subclavian veins (SV), left greater than right. The high signal intensity left external jugular vein (XJ) joined the internal jugular (J) and subclavian

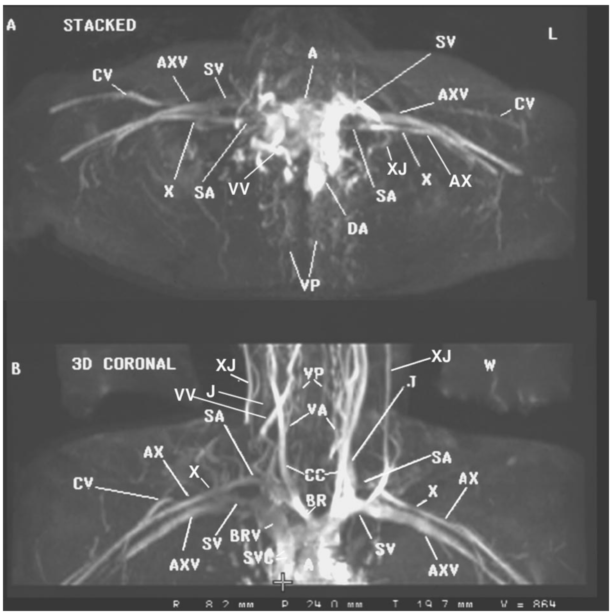

Figure 6(A,B). Figure 6A displays the two dimensional Time of Flight (2D TOF) MRA stacked image (arms at the side). The asymmetric forward rotated neurovascular blood supply, right anterior to left reflects the drooping smaller left shoulder and costoclavicular compression site (X)-between the diminished signal intensity of the subclavian veins (SV) and the proximally dilated axillosubclavian veins (AXV) with bilateral compression of the second division of the subclavian arteries (SA). Vertebral venous plexus of the spinal cord (VP); vertical attitude of the aorta (A) reflecting kyphosis of the thoracic spine; dilated right vertebral vein (VV), descending aorta (DA); vertebral vein (VV), cephalic vein (CV), left and right (L,R). Figure 6B displays a 3D coronal reconstructed image of the 2D TOF MRA (arms at the side), which cross references and confirms the stacked image (Fig.6A). The diminished signal intensities of the right internal jugular (J), external jugular (XJ), brachiocephalic (BRV), and subclavian (SV) veins reflect costoclavicular compression and edema within the right supraclavicular fossa and right neck as compared to left supraclavicular fossa. The smaller left subclavian artery (SA) is compressed within the scalene triangle, greater than the right subclavian artery. The dilated left axillosubclavian vein (AXV) is larger than the right axillosubclavian vein. Aorta (A), axillosubclavian artery (AX), cephalic vein (CV), common carotid arteries (CC), superior vena cava (SVC), vertebral arteries (VA), vertebral venous plexus of the spinal cord (VP); dilated right vertebral vein (VV), left and right (L,R), saline water bag (W), and site of costoclavicular compression (x).

vein (SV) medial and superior to the compressed bicuspid valve of the subclavian vein

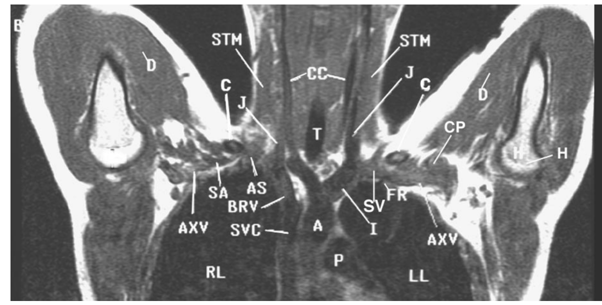

Figure 7. This is a coronal abduction external rotation MR image of the upper extremities (arms overhead). The clavicles (C) with the subclavius muscles and the coracoid processes (CP) enhance costoclavicular compression of the draining veins and lymphatics of the within the neck and supraclavicular fossa. Aorta (A), humerus (H), subclavian artery (SA), axillosubclavian, subclavian, brachiocephalic veins (AXV, SV, BRV), common carotid arteries (CC), first rib (FR), deltoid, sternocleidomastoid muscles (D, STM), superior vena cava (SVC), trachea (T), left and right lungs (L,R).

contributing to the proximal dilated left axillosubclavian vein (AXV). The elongated aorta (A) reflected kyphosis of the thoracic spine, and the dilated right vertebral vein (VV) reflected decreased venous return secondary to costoclavicular compression

The 3D coronal reconstructed images (Fig. 6B) confirmed the stacked image. Gray signal intensities of the right neck and shoulder venous drainage suggested greater costoclavicular compression on the right than left. The compression of the right internal jugular vein (J) cross referenced the transverse and right sagittal sequences above. However, the high signal intensity of the left external jugular vein (XJ) suggested increased collateral venous return. The proximally dilated left axillosubclavian vein (AXV) suggested greater focal compression of the bicuspid valve within the smaller left subclavian vein (SV) as compared to the right subclavian vein.

Bilateral coronal abduction external of the upper extremities posterior inferiorly rotated the clavicles (C) and subclavius muscles (SUB) with posterior anterior medial rotation of the coracoid processes (CP) enhancing costoclavicular compression as above described (Fig. 7).

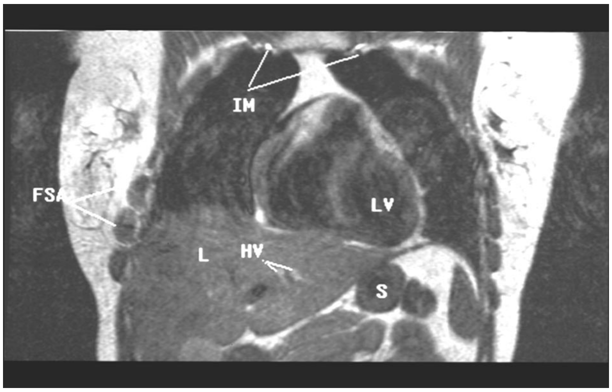

Figure 8. This is an anterior image of the coronal abduction external rotation of the upper extremities sequence in Figure 7. This image displays high signal intensity (white) internal mammary (IM) and hepatic veins (H) reflecting increased thoracic and abdominal pressure secondary to decreased venous return on a T-1 sequence. First fascicle of the serratus anterior muscle (FSA), liver (L), left ventricle (LV), stomach (S)

The low left clavicle with the subclavius muscle and the coracoid process markedly compressed the draining veins within the neck, supraclavicular fossae, and mildly compressed the neurovascular bundle, left greater than right. High signal intensity internal mammary (IM) and hepatic veins (H) (Fig. 8) displayed decreased venous return which caused increased intrathoracic, intraabdominal, and increased intracranial pressures[14].

Bilateral abduction external rotation of the upper extremities (arms overhead) triggered immediate pain with whole arm and hand numbness, left greater than right. Pain radiated from the shoulder, down the left triceps muscle to the elbow with bilateral throbbing frontal headache, and blurred vision. Abdomen and lower extremity complaints were not expressed.

She was informed of our findings and advised to discuss her problem with the referring physician. She sought a second opinion. The second opinion agreed with our findings of bilateral round shoulders, anterior compression of the mid-thoracic vertebrae (Fig. 2, 7T, 8T) accentuated by kyphosis of the thoracic spine; bilateral asymmetric costoclavicular compression (laxity of the erector muscles) of the draining veins within the neck, supraclavicular fossae (Ieft greater than right), mild compression of the neurovascular bundles. She was referred to vascular surgery for further evaluation for possible scalenectomy and left first rib resection[15]. Approximately 6 months later, she underwent transaxillary first rib, anterior and middle scalenectomy with neurolysis of the inferior trunk of the left brachial plexus. The left first rib was transected posteriorly to the transverse process and disarticulated from the stenochrondral junction. The sterochondral and steroclavicular ligaments, and the subclavius tendon were divided. The surgeon found a thick fibrous band originating on the middle scalene muscle, anterior to the subclavian artery, and inserting on to Sibson's fascia. The band was resected and removed and in doing so relieved compression and deviation of the T1 nerve root. She tolerated the procedure well and was discharged for follow up clinic visits. Following her scheduled recovery period, she was scheduled for physical therapy-specifically designed for TOS patients[16].

DISCUSSION

The PA and lateral upright chest radiographs in this patient displayed bilateral round shoulders, drooping right and anterior rotated left shoulder, and kyphosis of the thoracic spine accentuated by anterior wedging of the 7T and 8T vertebrae (Figs. 1,2). Multiplanar high resolution bilateral MRI sequences (supine position) cross referenced and confirmed thin narrow fascial planes posterior to the clavicles and subclavius muscles, and drooping (laxity of the erector/sling muscles) of the smaller left shoulder (Figs. 3,4); costoclavicular compression of the subclavian veins in the neutral position (Fig. 4), and the forward shift of the cervicothoracic spine (Fig. 5A). The 2D TOF MRA and 3D reconstructed coronal images documented compression of the draining veins of the neck, supraclavicular fossae and mild compression of the subclavian arteries with binding nerve roots (Figs. 6A,B). The abduction external rotation of the upper extremity sequence (arms overhead) enhanced costoclavicular compression, greater left than right (Fig. 7), and captured images displaying the high signal intensity (white) of obstructed flow within the hepatic and internal mammary veins on the T1 weighted sequence. Triggered complaints of headache, blurred vision, and ringing in the ears reflected costoclavicular compression, left greater than right[13].

Structural changes in the alignment of the cervicothoracic spine as with kyphosis in this patient; aging; injuries; illnesses; sedentary life styles, and restricted movements with muscle disuse contribute to atrophy of muscles and soft tissues[16]. Laxity of the shoulder muscles contribute to costoclavicular compression of the venous drainage within the neck, supraclavicular fossae, and of the neurovascular bundles[17].

The circulatory system is a closed system. Compression of the venous drainage from peripheral nerves, impedes venous and lymphatic return, and in turn increases arterial pressure. Valves are located within veins and lymphatics to support, assist and direct blood and lymph flow. A bicuspid valve is located near the termination of the internal jugular vein as it joins the subclavian vein to form the brachiocephalic and innominate veins. A bicuspid valve (anterior and posterior cusps) is usually located lateral to opening of the external jugular vein[13]. If external pressure is applied to the upper extremity, the walls of the draining veins and lymphatics may compress the valves within. Surface veins may be observed to dilate reflecting lymph and venous blood back up within soft tissues and nerves. Arterial blood flow is impeded. This inturn may cause increase in intrathoracic, intraabdominal, and intravascular pressures[14].

The simple inflation of a blood pressure cuff, with preserved radial and brachial pulses, may be visually observed to obstruct the draining veins of the upper extremities in patients without TOS. They may complain of increased pressure in their hands and arms; tingling, numbness, and throbbing pain; discoloration of the fingers and hand; dizzy and light headed sensations with headaches, and blurred vision with swooshing and ringing in the ears[11,17,18]. The longer the obstruction, the greater the complaints. Triggered complaints reflect venous obstruction below the blood pressure cuff, tourniquet or when hands are applied to squeeze the upper arm[19]. This venous compression interrupts the local blood supply from the nerve fibers causing numbness, weakness, pain, and decreased signal conduction velocity. Transient or permanent compression ischemia if unrelieved progressively affect the nerve fibers in increasing numbers and to an increasing degree. Pathology develops with edematous swelling and vascular congestion. If the pressure is unrelieved and continues to increase, the nerve(s) suffer a first degree or conduction block injury. Compression ischemia with degeneration and fibrosis develop. In absence of relief, the endoneurial tubes and funniculi atrophy and with increasing ischemia, fibrosis becomes marked[20].

Round shoulders (laxity) associated with kyphosis of the thoracic spine cause costoclavicular venous compression and brachial plexopathy[21]. This form of thoracic outlet syndrome is usually not amenable to surgical treatment in the older patients, particularly in severe kyphosis of the thoracic spine[9,10].

"You only see what you know"

We have imaged over 3000 patients presenting with symptoms of TOS reflecting compromising or compression abnormalities of the brachial plexus. It is instructive that these patients have a common MRI/MRA finding, costoclavicular compression of the draining veins within the neck and supraclavicular fossae triggering complaints as above described[17,19,21,22,23].

Other possible etiologies of the patient's complaints were ruled out by the MRI/MRA. Our narrative presentation included statements and descriptions of images not displayed. A more extensive report for the patient's file was supported by all of the sequences including the above selected images. Unlike x-ray images, a diagnosis is not made from a single plain film[8,23], although chest radiographs are correlated with the MRI and MRA for a more accurate diagnosis[20]. Since it is not possible to present all of the images, those selected best demonstrated the pathology[11,19,21,24,25,26].

LITERATURE CITED

1. Collins JD, Batra P, Brown K, Shaver M.L. Anatomy of the thorax and shoulder girdle as displayed by magnetic resonance imaging. *J Natl Med Assoc.*1991;83:46–52.

2. Collins JD, Batra P, Brown K, Shaver ML. Anatomy of the thorax and shoulder girdle as displayed by magnetic resonance imaging. *Anat. Rec.* 1986;214:24A.

3. Collins JD, Saxton EH, Ahn SS, Miller TQ. The role of the Manubrium sterni, clavicle and subclavius muscle, and scapula in venous obstruction of the brachial plexus:MRI and MRA. *Clin Anat* 1999;12:435.

4. Sunderland S. Blood supply of the nerves to the upper limb in man. *Arch Neurol Psych.*1945;53:91–115.

5. Dyck PK, Barnes J, Lais L. Pathological alterations of the peripheral nervous system of humans: Peripheral Neuropathy. ed. 2. Philadelphia, WB Saunders Co, 1984;760–870.

6. Collins JD, Saxton EH, Ahn SS, Miller TQ, Carnes AE, Newkirk TA. The vascular supply of the brachial plexus as displayed by magnietic resonance angiography (MRA) cross referenced to MRI in patients with thoracic outlet syndrome. *FASEB* 2002;16:A380.

7. Collins JD, Disher A, Miller TQ. The vascular supply of the brachial plexus as displayed by magnetic resonance imaging: magnetic resonance angiography (MRA). *Clin Anat* 1995;2:155.

8. Schinz HR, Baensch WE, Frommhold W, Glauner R, Uehlinger E, Wellauer J. Roentgen Diagnosis. 1969;3:32–37.

9. Collins JD, Saxton EH, Miller TQ, Ahn SS. Scheuermann's disease: A model displaying the mechanism of venous obstruction in thoracic outlet syndrome and Migraine patients; MRI and MRA, Presented at the National Medical Association 104th Annual Scientific Program, Convention and Scientific Assembly, Convention center, Las Vegas, Nevada, August 11, 1999.

10. Collins JD, Saxton E, Miller TQ, Ahn SS. Scheuermann's disease: A model displaying the mechanism of venous obstruction in thoracic outlet syndrome and migraine patients; MRI and MRA. *FASEB* 2000;14:A310.

11. Saxton EH, Collins JD, Miller TQ, Espinoza A. Migraine complicated by brachial plexopathy as displayed by MRI and MRA: Aberrant subclavian artery and cervical ribs. *J. Nat. Med. Assoc.*1999;91:333–341.

12. www.tosinfo.com Thoracic Outlet Syndrome (TOS) Information. Website designed by Ramona Tung, 2002.

13. Woodburne RT, Burkel WE. Essentials of Human Anatomy. ed. 8th. New York, Oxford University Press 1988;18–216.

14. Best CH, Taylor NB. The physiologiacal basis of medical practice. Ed 6th. Baltimore, The Williams & Wilkins Co.1955; 152–174.

15. Machleder HI. Transaxillary operative management of thoracic outlet syndrome. Current therapy in vascular supply B.C. Decker Incorporated, 1991;227–230.

16. Lord JW. Critical reappraisal of diagnostic and therapeutic modalities for thoracic outlet syndromes. Surgery, Gynecology and Obstetrics.1989;168:337–340.

17. Collins JD, Disher A, Miller TQ, Shaver ML. The costoclavicular syndrome as displayed by MRI and MRA: Reformat and 3D graphic display compromising brachioplexopathy *Clin Anat*, 1997;10:131.

18. Saxton EH, Collins JD, Miller TQ, Espinoza A. Migraine complicated by brachial plexopathy as displayed by MRI and MRA: Aberrant subclavian artery and cervical ribs. *FASEB* 1998; 12:A1110.

19. Collins JD, Saxton EH, Miller TQ, Ahn SS. Venous obstruction in Sphygmomanometric (BP) measurement causes numbness and tingling; MRI and MRA.*FASEB* 2000;14:A310.

20. Sunderland S. Nerves and Nerve Injuries, Baltimore, Williams & Wilkins Co.,1968.

21. Collins JD, Shaver ML, Disher A, Miller TQ. Compromising abnormalities of the brachial plexus as displayed by magnetic resonance imaging. *Clin. Anat.*1995;8:1–16.

22. Collins JD, Disher A, Miller TQ. The vascular supply of the brachial plexus as displayed by magnetic resonance imaging: Magnetic resonance Angiography (MRA). *Clin Anat* 1995;2:155.

23. Saxton EH, Miller TQ, Collins JD. Neurovascular compression on MRI in patients with intractable migraine. Cephalalgia 1999;19:330–301.

24. Collins JD, Shaver ML, Disher AC, Miller TQ. Bilateral magnetic resonance imaging of the brachial plexus and peripheral nerve imaging: Technique and three-dimensional color. In Management of Peripheral Nerve Problems. Omer, G.E., M. Spinner and A.L.Van Beek (ed.). 2nd ed, W.B. Saunders Co., 1998;82–93.

25. Saxton EH, Miller TQ, Collins JD. Migraine complicated by brachial plexopathy as displayed by MRI and MRA: Aberrant subclavian artery and cervical ribs. Neurology Reviews, 2001;1:8–11.

26. Tung RH. (2002). Thoracic Outlet Syndrome (TOS) information. Retrieved October 17, 2002, http://tosinfo.com/

We Welcome Your Comments

Journal of the National Medical Association welcomes your Letters to the Editor about articles that appear in the *JNMA* or issues relevant to minority health care.

Address correspondence to Editor-in-Chief, *JNMA*, 1012 Tenth St, NW, Washington, DC 20001; fax (202) 371-1162; or ktaylor @nmanet.org.